

**Identified hadron spectra at large transverse
momentum in $p+p$ and $d+Au$ collisions at
 $\sqrt{s_{NN}} = 200 \text{ GeV}$**

J. Adams^b, M.M. Aggarwal^{ac}, Z. Ahammed^{ar}, J. Amonett^s,
 B.D. Anderson^s, M. Anderson^f, D. Arkhipkin^l,
 G.S. Averichev^k, S.K. Badyal^r, Y. Bai^{aa}, J. Balewski^p,
 O. Barannikova^{af}, L.S. Barnby^b, J. Baudot^q, S. Bekele^{ab},
 V.V. Belaga^k, A. Bellingeri-Laurikainen^{am}, R. Bellwied^{au},
 B.I. Bezverkhny^{aw}, S. Bharadwaj^{ah}, A. Bhasin^r, A.K. Bhati^{ac},
 H. Bichsel^{at}, J. Bielcik^{aw}, J. Bielcikova^{aw}, A. Billmeier^{au},
 L.C. Bland^c, C.O. Blyth^b, S-L. Blyth^u, B.E. Bonner^{ai},
 M. Botje^{aa}, J. Bouchet^{am}, A.V. Brandin^y, A. Bravar^c,
 M. Bystersky^j, R.V. Cadman^a, X.Z. Cai^{al}, H. Caines^{aw},
 M. Calderón de la Barca Sánchez^f, J. Castillo^{aa}, O. Catu^{aw},
 D. Cebra^f, Z. Chajecki^{ab}, P. Chaloupka^j, S. Chattopadhyay^{ar},
 H.F. Chen^{ak}, J.H. Chen^{al}, Y. Chen^g, J. Cheng^{ap}, M. Cherneyⁱ,
 A. Chikanian^{aw}, H.A. Choi^{ag}, W. Christie^c, J.P. Coffin^q,
 T.M. Cormier^{au}, M.R. Cosentino^{aj}, J.G. Cramer^{at},
 H.J. Crawford^e, D. Das^{ar}, S. Das^{ar}, M. Daugherty^{ao},
 M.M. de Moura^{aj}, T.G. Dedovich^k, M. DePhillips^c,
 A.A. Derevschikov^{ae}, L. Didenko^c, T. Dietel^m, P. Djawotho^p,
 S.M. Dogra^r, W.J. Dong^g, X. Dong^{ak}, J.E. Draper^f, F. Du^{aw},
 V.B. Dunin^k, J.C. Dunlop^c, M.R. Dutta Mazumdar^{ar},
 V. Eckardt^w, W.R. Edwards^u, L.G. Efimov^k, V. Emelianov^y,
 J. Engelage^e, G. Eppley^{ai}, B. Erazmus^{am}, M. Estienne^q,
 P. Fachini^c, R. Fatemi^v, J. Fedorisin^k, K. Filimonov^u,
 P. Filip^j, E. Finch^{aw}, V. Fine^c, Y. Fisyak^c, K.S.F. Fornazier^{aj},
 J. Fu^{av}, C.A. Gagliardi^{an}, L. Gaillard^b, J. Gans^{aw},
 M.S. Ganti^{ar}, V. Ghazikhanian^g, P. Ghosh^{ar}, J.E. Gonzalez^g,
 Y.G. Gorbunovⁱ, H. Gos^{as}, O. Grachov^{au}, O. Grebenyuk^{aa},
 D. Grosnick^{aq}, S.M. Guertin^g, Y. Guo^{au}, A. Gupta^r,
 N. Gupta^r, T.D. Gutierrez^f, B. Haag^f, T.J. Hallman^c,

A. Hamed^{au}, J.W. Harris^{aw}, W. He^p, M. Heinz^{aw},
 T.W. Henry^{an}, S. Hepplemann^{ad}, B. Hippolyte^q, A. Hirsch^{af},
 E. Hjort^u, G.W. Hoffmann^{ao}, M.J. Horner^u, H.Z. Huang^g,
 S.L. Huang^{ak}, E.W. Hughes^d, T.J. Humanic^{ab}, G. Igo^g,
 P. Jacobs^u, W.W. Jacobs^p, P. Jakl^j, F. Jia^t, H. Jiang^g,
 P.G. Jones^b, E.G. Judd^e, S. Kabana^{am}, K. Kang^{ap},
 J. Kapitan^j, M. Kaplan^h, D. Keane^s, A. Kechechyan^k,
 V.Yu. Khodyrev^{ae}, B.C. Kim^{ag}, J. Kiryluk^v, A. Kisiel^{as},
 E.M. Kislov^k, S.R. Klein^u, D.D. Koetke^{aq}, T. Kollegger^m,
 M. Kopytine^s, L. Kotchenda^y, V. Kouchpil^j, K.L. Kowalik^u,
 M. Kramer^z, P. Kravtsov^y, V.I. Kravtsov^{ae}, K. Krueger^a,
 C. Kuhn^q, A.I. Kulikov^k, A. Kumar^{ac}, A.A. Kuznetsov^k,
 M.A.C. Lamont^{aw}, J.M. Landgraf^c, S. Lange^m, F. Laue^c,
 J. Lauret^c, A. Lebedev^c, R. Lednicky^k, C-H. Lee^{ag},
 S. Lehocka^k, M.J. LeVine^c, C. Li^{ak}, Q. Li^{au}, Y. Li^{ap}, G. Lin^{aw},
 S.J. Lindenbaum^z, M.A. Lisa^{ab}, F. Liu^{av}, H. Liu^{ak}, J. Liu^{ai},
 L. Liu^{av}, Z. Liu^{av}, T. Ljubicic^c, W.J. Llope^{ai}, H. Long^g,
 R.S. Longacre^c, M. Lopez-Noriega^{ab}, W.A. Love^c, Y. Lu^{av},
 T. Ludlam^c, D. Lynn^c, G.L. Ma^{al}, J.G. Ma^g, Y.G. Ma^{al},
 D. Magestro^{ab}, S. Mahajan^r, D.P. Mahapatraⁿ, R. Majka^{aw},
 L.K. Mangotra^r, R. Manweiler^{aq}, S. Margetis^s, C. Markert^s,
 L. Martin^{am}, H.S. Matis^u, Yu.A. Matulenko^{ae}, C.J. McClain^a,
 T.S. McShaneⁱ, Yu. Melnick^{ae}, A. Meschanin^{ae}, M.L. Miller^v,
 N.G. Minaev^{ae}, S. Mioduszewski^{an}, C. Mironov^s, A. Mischke^{aa},
 D.K. Mishraⁿ, J. Mitchell^{ai}, B. Mohanty^{ar}, L. Molnar^{af},
 C.F. Moore^{ao}, D.A. Morozov^{ae}, M.G. Munhoz^{aj}, B.K. Nandi^o,
 S.K. Nayak^r, T.K. Nayak^{ar}, J.M. Nelson^b, P.K. Netrakanti^{ar},
 V.A. Nikitin^l, L.V. Nogach^{ae}, S.B. Nurushev^{ae}, G. Odyniec^u,
 A. Ogawa^c, V. Okorokov^y, M. Oldenburg^u, D. Olson^u,
 M. Pachr^j, S.K. Pal^{ar}, Y. Panebratsev^k, S.Y. Panitkin^c,
 A.I. Pavlinov^{au}, T. Pawlak^{as}, T. Peitzmann^{aa},
 V. Perevoztchikov^c, C. Perkins^e, W. Peryt^{as}, V.A. Petrov^{au},
 S.C. Phatakⁿ, R. Picha^f, M. Planinic^{ay}, J. Pluta^{as},
 N. Poljak^{ay}, N. Porile^{af}, J. Porter^{at}, A.M. Poskanzer^u,
 M. Potekhin^c, E. Potrebenikova^k, B.V.K.S. Potukuchi^r,

D. Prindle^{at}, C. Pruneau^{au}, J. Putschke^u, G. Rakness^{ad},
 R. Raniwala^{ah}, S. Raniwala^{ah}, R.L. Ray^{ao}, S.V. Razin^k,
 J. Reinnarth^{am}, D. Relyea^d, F. Retiere^u, A. Ridiger^y,
 H.G. Ritter^u, J.B. Roberts^{ai}, O.V. Rogachevskiy^k,
 J.L. Romero^f, A. Rose^u, C. Roy^{am}, L. Ruan^u,
 M.J. Russcher^{aa}, R. Sahooⁿ, I. Sakrejda^u, S. Salur^{aw},
 J. Sandweiss^{aw}, M. Sarsour^{an}, I. Savin^l, P.S. Sazhin^k,
 J. Schambach^{ao}, R.P. Scharenberg^{af}, N. Schmitz^w,
 K. Schweda^u, J. Segerⁱ, I. Selyuzhenkov^{au}, P. Seyboth^w,
 A. Shabetai^u, E. Shahaliev^k, M. Shao^{ak}, M. Sharma^{ac},
 W.Q. Shen^{al}, S.S. Shimanskiy^k, E. Sichtermann^u, F. Simon^v,
 R.N. Singaraju^{ar}, N. Smirnov^{aw}, R. Snellings^{aa}, G. Sood^{aq},
 P. Sorensen^c, J. Sowinski^p, J. Speltz^q, H.M. Spinka^a,
 B. Srivastava^{af}, A. Stadnik^k, T.D.S. Stanislaus^{aq}, R. Stock^m,
 A. Stolpovsky^{au}, M. Strikhanov^y, B. Stringfellow^{af},
 A.A.P. Suaide^{aj}, E. Sugarbaker^{ab}, M. Sumbera^j, Z. Sun^t,
 B. Sorrow^v, M. Swangerⁱ, T.J.M. Symons^u,
 A. Szanto de Toledo^{aj}, A. Tai^g, J. Takahashi^{aj}, A.H. Tang^c,
 T. Tarnowsky^{af}, D. Thein^g, J.H. Thomas^u, A.R. Timmins^b,
 S. Timoshenko^y, M. Tokarev^k, T.A. Trainor^{at}, S. Trentalange^g,
 R.E. Tribble^{an}, O.D. Tsai^g, J. Ulery^{af}, T. Ullrich^c,
 D.G. Underwood^a, G. Van Buren^c, N. van der Kolk^{aa},
 M. van Leeuwen^u, A.M. Vander Molen^x, R. Varma^o,
 I.M. Vasilevski^l, A.N. Vasiliev^{ae}, R. Vernet^q, S.E. Vigdor^p,
 Y.P. Viyogi^{ar}, S. Vokal^k, S.A. Voloshin^{au}, W.T. Waggonerⁱ,
 F. Wang^{af}, G. Wang^s, J.S. Wang^t, X.L. Wang^{ak}, Y. Wang^{ap},
 J.W. Watson^s, J.C. Webb^p, G.D. Westfall^x, A. Wetzler^u,
 C. Whitten Jr.^g, H. Wieman^u, S.W. Wissink^p, R. Witt^{aw},
 J. Wood^g, J. Wu^{ak}, N. Xu^u, Q.H. Xu^u, Z. Xu^c, P. Yepes^{ai},
 I-K. Yoo^{ag}, V.I. Yurevich^k, I. Zborovsky^j, W. Zhan^t,
 H. Zhang^c, W.M. Zhang^s, Y. Zhang^{ak}, Z.P. Zhang^{ak},
 Y. Zhao^{ak}, C. Zhong^{al}, R. Zoulkarneev^l, Y. Zoulkarneeva^l,
 A.N. Zubarev^k and J.X. Zuo^{al}

(STAR Collaboration)

^aArgonne National Laboratory, Argonne, Illinois 60439

- ^b *University of Birmingham, Birmingham, United Kingdom*
- ^c *Brookhaven National Laboratory, Upton, New York 11973*
- ^d *California Institute of Technology, Pasadena, California 91125*
- ^e *University of California, Berkeley, California 94720*
- ^f *University of California, Davis, California 95616*
- ^g *University of California, Los Angeles, California 90095*
- ^h *Carnegie Mellon University, Pittsburgh, Pennsylvania 15213*
- ⁱ *Creighton University, Omaha, Nebraska 68178*
- ^j *Nuclear Physics Institute AS CR, 250 68 Řež/Prague, Czech Republic*
- ^k *Laboratory for High Energy (JINR), Dubna, Russia*
- ^l *Particle Physics Laboratory (JINR), Dubna, Russia*
- ^m *University of Frankfurt, Frankfurt, Germany*
- ⁿ *Institute of Physics, Bhubaneswar 751005, India*
- ^o *Indian Institute of Technology, Mumbai, India*
- ^p *Indiana University, Bloomington, Indiana 47408*
- ^q *Institut de Recherches Subatomiques, Strasbourg, France*
- ^r *University of Jammu, Jammu 180001, India*
- ^s *Kent State University, Kent, Ohio 44242*
- ^t *Institute of Modern Physics, Lanzhou, P.R. China*
- ^u *Lawrence Berkeley National Laboratory, Berkeley, California 94720*
- ^v *Massachusetts Institute of Technology, Cambridge, MA 02139-4307*
- ^w *Max-Planck-Institut für Physik, Munich, Germany*
- ^x *Michigan State University, East Lansing, Michigan 48824*
- ^y *Moscow Engineering Physics Institute, Moscow Russia*
- ^z *City College of New York, New York City, New York 10031*
- ^{aa} *NIKHEF and Utrecht University, Amsterdam, The Netherlands*
- ^{ab} *Ohio State University, Columbus, Ohio 43210*
- ^{ac} *Panjab University, Chandigarh 160014, India*
- ^{ad} *Pennsylvania State University, University Park, Pennsylvania 16802*
- ^{ae} *Institute of High Energy Physics, Protvino, Russia*
- ^{af} *Purdue University, West Lafayette, Indiana 47907*
- ^{ag} *Pusan National University, Pusan, Republic of Korea*
- ^{ah} *University of Rajasthan, Jaipur 302004, India*
- ^{ai} *Rice University, Houston, Texas 77251*
- ^{aj} *Universidade de Sao Paulo, Sao Paulo, Brazil*
- ^{ak} *University of Science & Technology of China, Hefei 230026, China*

^{al}*Shanghai Institute of Applied Physics, Shanghai 201800, China*

^{am}*SUBATECH, Nantes, France*

^{an}*Texas A&M University, College Station, Texas 77843*

^{ao}*University of Texas, Austin, Texas 78712*

^{ap}*Tsinghua University, Beijing 100084, China*

^{aq}*Valparaiso University, Valparaiso, Indiana 46383*

^{ar}*Variable Energy Cyclotron Centre, Kolkata 700064, India*

^{as}*Warsaw University of Technology, Warsaw, Poland*

^{at}*University of Washington, Seattle, Washington 98195*

^{au}*Wayne State University, Detroit, Michigan 48201*

^{av}*Institute of Particle Physics, CCNU (HZNU), Wuhan 430079, China*

^{aw}*Yale University, New Haven, Connecticut 06520*

^{ay}*University of Zagreb, Zagreb, HR-10002, Croatia*

Abstract

We present the transverse momentum (p_T) spectra for identified charged pions, protons and anti-protons from $p+p$ and $d+Au$ collisions at $\sqrt{s_{NN}} = 200$ GeV. The spectra are measured around midrapidity ($|y| < 0.5$) over the range of $0.3 < p_T < 10$ GeV/ c with particle identification from the ionization energy loss and its relativistic rise in the Time Projection Chamber and Time-of-Flight in STAR. The charged pion and proton+anti-proton spectra at high p_T in $p+p$ and $d+Au$ collisions are in good agreement with a phenomenological model (EPOS) and with next-to-leading order perturbative quantum chromodynamic (NLO pQCD) calculations with a specific fragmentation scheme and factorization scale. We found that all proton, anti-proton and charged pion spectra in $p+p$ collisions follow x_T -scaling for the momentum range where particle production is dominated by hard processes ($p_T \gtrsim 2$ GeV/ c). The nuclear modification factor around midrapidity is found to be greater than unity for charged pions and to be even larger for protons at $2 < p_T < 5$ GeV/ c .

Key words: Particle production, perturbative quantum chromodynamics, fragmentation function, Cronin effect and x_T -scaling.

1 Introduction

The study of identified hadron spectra at large transverse momentum (p_T) in $p+p$ collisions can be used to test the predictions from perturbative quantum chromodynamics (pQCD) [1]. In the framework of models based on QCD, the inclusive production of single hadrons is described by the convolution of

parton distribution functions (PDFs), parton interaction cross-sections and fragmentation functions (FFs). The PDF provide the probability of finding a parton (a quark or a gluon) in a hadron as a function of the fraction of the hadron's momentum carried by the parton. The FFs [2] give the probability for a hard scattered parton to fragment into a hadron of a given momentum fraction. These are not yet calculable from the first principles and hence are generally obtained from experimental data (e.g., e^+e^- collisions). The factorization theorem for cross-sections assumes that FFs are independent of the process in which they have been determined and hence represent a universal property of hadronization. It is therefore possible to make quantitative predictions for other types of collision systems (e.g., $p+p$). Comparisons between experimental data and theory can help to constrain the quark and gluon FFs that are critical to predictions of hadron spectra in $p+p$, $p+A$, and $A+A$ collisions. The simultaneous study of identified hadron p_T spectra in $p+p$ and $d+Au$ collisions may also provide important information on the PDFs [3] of the nucleus.

The identified particle spectra in $p+p$ and $d+Au$ collisions also provide reference spectra for particle production at high p_T in $Au+Au$ collisions. Moreover, studies of identified particle production and their ratios as a function of p_T in high-energy heavy-ion collisions have revealed many unique features in different p_T regions [4–7] and between baryons and mesons [8]. A good description of both identified pion and proton spectra in $p+p$ and $d+Au$ collisions at intermediate and high p_T by NLO pQCD will provide a solid ground for models based on jet quenching [9] and quark recombination [6]. These emphasize the need for a systematic study of p_T spectra from $p+p$ and $d+Au$ collisions at the same energy as the nucleus-nucleus collisions.

In this letter, we present the p_T spectra for identified pions, protons and anti-protons in $p+p$ and $d+Au$ collisions at $\sqrt{s_{NN}} = 200$ GeV as measured by the STAR experiment at RHIC. The results are compared to NLO pQCD calculations and a phenomenological model. We also study the x_T -scaling in $p+p$ collisions and the nuclear modification factors in $d+Au$ collisions.

2 Experiment and Analysis

The STAR experiment consists of several detectors to measure hadronic and electromagnetic observables spanning a large region of the available phase space at RHIC. The detectors used in the present analysis are the Time Projection Chamber (TPC), the Time-Of-Flight (TOF) detector, a set of trigger detectors used for obtaining the minimum bias data, and the Forward Time Projection Chamber for the collision centrality determination in $d+Au$ collisions. The details of the design and other characteristics of the detectors can

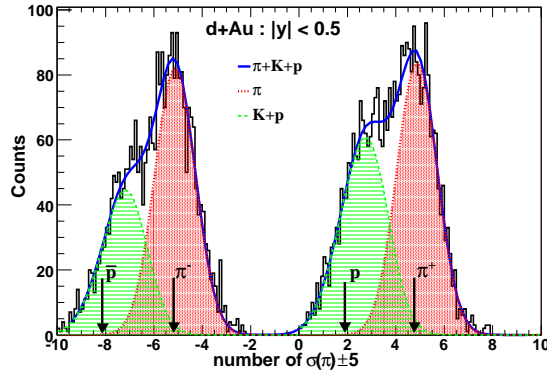


Fig. 1. dE/dx distribution normalized by pion dE/dx at $4.5 < p_T < 5.0$ GeV/ c and $|\eta| < 0.5$, and shifted by ± 5 for positively and negatively charged particles, respectively. The distributions are for minimum bias d +Au collisions. The pion, proton and anti-proton peak positions are indicated by arrows.

be found in Ref. [10].

A total of 8.2 million minimum bias $p+p$ collision events and 11.7 million d +Au collision events have been analyzed for the present study. The data set was collected during the years 2001 and 2003. The details of minimum bias trigger conditions for $p+p$ and d +Au collisions can be found in the Refs. [11,12]. The minimum-bias trigger captured $95 \pm 3\%$ of the 2.21 ± 0.09 barn d +Au inelastic cross-section. The trigger efficiency was determined from a cross study of two sets of trigger detectors: two Zero-Degree Calorimeters (ZDCs) and two beam-beam counters (BBCs). The absolute cross-section is derived from a Monte Carlo Glauber calculation. These results are consistent with other recent measurements [13]. The trigger for the minimum bias $p+p$ collisions required a coincidence measurement of the two BBCs covering $3.3 < |\eta| < 5.0$ [14]. This trigger was sensitive to color exchange hadronic and doubly-diffractive events; here, these are labelled "non-singly diffractive (NSD) events". Using PYTHIA(v6.205) [15] and HERWIG [16], it was determined that the trigger measured 87% of the 30.0 ± 3.5 mb NSD cross-section, which was measured via a vernier scan [17]. The data from TOF are used to obtain the identified hadron spectra for $p_T < 2.5$ GeV/ c . The procedure for particle identification in TOF has been described in Ref. [18]. For $p_T > 2.5$ GeV/ c , we use data from the TPC. Particle identification at high p_T in the TPC comes from the relativistic rise of the ionization energy loss (dE/dx). Details of the method are described in Ref. [19]. At $p_T \gtrsim 3$ GeV/ c , the pion dE/dx is about 10–20% higher than that of kaons and protons due to the relativistic rise, resulting in a few standard deviations (1 - 3σ) separation between them. Since pions are the dominant component of the hadrons in $p+p$ and d +Au collisions at RHIC, the prominent pion peak in the dE/dx distribution is fit with a Gaussian to extract the pion yield [19]. The proton yield is obtained by integrating the entries (Y) in the low part of the dE/dx distribution about 2.5σ away from

the pion dE/dx peak. The integration limits were varied to check the stability of the results. Fig. 1 shows a typical dE/dx distribution normalized by the pion dE/dx at $4.5 < p_T < 5.0$ GeV/ c and $|\eta| < 0.5$. The Gaussian distribution used to extract the pion yield and the pion, proton and anti-proton peak positions are also shown in the figure.

The kaon contamination is estimated via either of the equations given below. The uncorrected proton yield is

$$p = (Y - \beta(h - \pi))/(\alpha - \beta)$$

or

$$p = (Y - \beta K_S^0)/\alpha,$$

where α and β are the proton and kaon efficiencies from the integration described above, derived from the dE/dx calibration, resolution and the Bichsel function [19,20]. In the first case the kaon contamination is estimated through the yields of the inclusive hadrons (h) and pions, in case two from known yields from K_S^0 measurements [19,21]. The typical values of α for a dE/dx cut slightly away from the proton peak position is 0.4 and the β values decrease from 0.2 to 0.08 with p_T in the range $2.5 < p_T < 10$ GeV/ c . At high p_T , the yields of other stable particles (i.e., electrons and deuterons) are at least two orders of magnitude lower than those of pions, and are negligible in our studies. The two results are consistent where STAR K_S^0 measurements are available. The p_T -dependence of the reconstruction efficiency, background and the systematic uncertainties for pions, protons and anti-protons for low p_T in $p+p$ and $d+Au$ collisions are described in Ref. [18]. At high p_T (> 2.5 GeV/ c), the efficiency is almost independent of p_T in both $p+p$ and $d+Au$ collisions. The tracking efficiencies are $\sim 88\%$ and 92% in $p+p$ and $d+Au$ collisions, respectively. The difference in tracking efficiency arises because of worse vertex determination in $p+p$ collisions than $d+Au$ collisions. The background contamination to pion spectra for $p_T > 2.5$ GeV/ c , primarily from K_S^0 weak decay is estimated from PYTHIA/HIJING simulations with full GEANT detector descriptions to be $\sim 4\%$. The charged pion spectra are corrected for efficiency and background effects. The inclusive proton and anti-proton spectra are presented with efficiency corrections and without hyperon feed-down corrections. The integrated Λ/p -ratio is estimated to be $< 25\%$ [18,21]. Additional corrections are applied for primary vertex reconstruction inefficiency as discussed in Refs. [11,12,18]. The momentum resolution is given as $\Delta p_T/p_T = 0.01 + 0.005p_T/(\text{GeV}/c)$ and has $< 4\%$ effect on the yields at the highest p_T value. The spectra are not corrected for momentum resolution effects, but they are included in the systematic errors.

The total systematic uncertainties associated with pion yields are estimated to be $\lesssim 15\%$. This systematic uncertainty is dominated by the uncertainty in modeling the detector response in the Monte Carlo simulations. Protons from

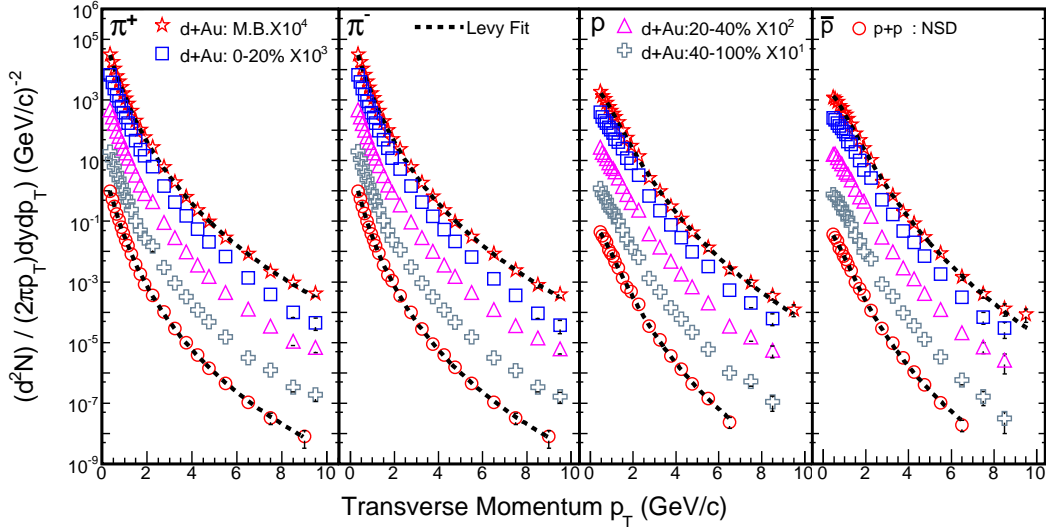


Fig. 2. Midrapidity ($|y| < 0.5$) transverse momentum spectra for charged pions, proton and anti-proton in $p+p$ and $d+Au$ collisions for various event centrality classes. Minimum bias distributions are fit to Levy functions which are shown as dashed curves.

hyperon (Λ and Σ) decays away from the primary vertex can be reconstructed as primordial protons at a slightly higher p_T than their true value, but with worse momentum resolution. This results in an uncertainty of the inclusive proton yield of $\sim 2\%$ at $p_T = 3$ GeV/ c and $\sim 10\%$ at $p_T = 10$ GeV/ c . For proton and anti-proton yields at high p_T an additional systematic error arises from the uncertainties in the determination of the efficiencies, α and β , under a specific dE/dx selection for integration. This is due to the uncertainties in the mean dE/dx positions for protons and kaons. The total systematic uncertainty in obtaining the proton and anti-proton yields for $p_T > 2.5$ GeV/ c increases with p_T from 12% to 23% (at $p_T = 10$ GeV/ c) in both $p+p$ and $d+Au$ collisions. The errors shown in the figures are statistical, and the systematic errors are plotted as shaded bands. In addition, there are overall normalization uncertainties from trigger and luminosity in $p+p$ and $d+Au$ collisions of 14% and 10%, respectively [11]. These errors are not shown.

Figure 2 shows the invariant yields of charged pions, protons and anti-protons for the p_T range of $0.3 < p_T < 10$ GeV/ c in minimum bias $p+p$ collisions and for various centrality classes in $d+Au$ collisions. The yields span over eight orders of magnitude. The minimum bias distributions are fit with a Levy distribution [22] of the form $\frac{d^2N}{2\pi p_T dp_T dy} = \frac{B}{(1+(m_T-m_0)/nT)^n}$, where $m_T = \sqrt{p_T^2 + m_0^2}$ and m_0 is the mass of the hadron. The Levy distribution essentially takes a power-law form at higher p_T and has an exponential form at low p_T . For the p and \bar{p} spectra, fit with a power-law function gives a worse χ^2/ndf compared to the fit with the Levy function. For $d+Au$ collisions the χ^2/ndf for the power-law fit to $p(\bar{p})$ spectra is 68.55/20(86.77/20) and the corresponding

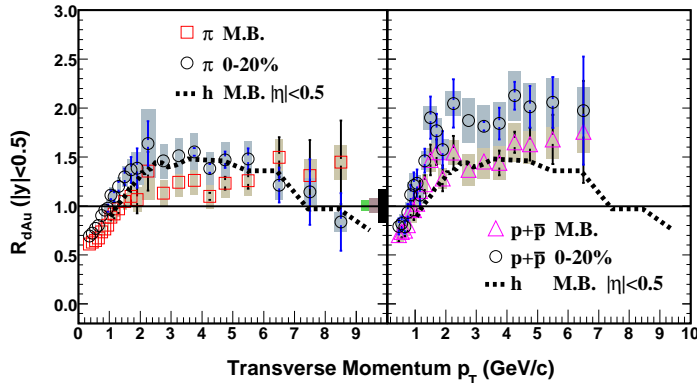


Fig. 3. Nuclear modification factors, R_{dAu} , for charged pions $\pi^+ + \pi^-$ and $p+\bar{p}$ at $|y| < 0.5$ in minimum bias and 0-20% central $d+Au$ collisions. For comparison results on inclusive charged hadrons (STAR) from Ref. [11] at $|\eta| < 0.5$ are shown by dashed curves. The first two shaded bands around 1 correspond to the error due to uncertainties in estimating the number of binary collisions in minimum bias and 0-20% central $d+Au$ collisions respectively. The last shaded band is the normalization uncertainty from trigger and luminosity in $p+p$ and $d+Au$ collisions.

value for the fit with the Levy function is 21.19/20(26.4/20).

3 Nuclear modification factor

The nuclear modification factor (R_{dAu}) can be used to study the effects of cold nuclear matter on particle production. It is defined as a ratio of the invariant yields of the produced particles in $d+Au$ collisions to those in $p+p$ collisions scaled by the underlying number of nucleon-nucleon binary collisions.

$$R_{dAu}(p_T) = \frac{d^2 N_{dAu}/dydp_T}{\langle N_{bin} \rangle / \sigma_{pp}^{inel} \cdot d^2 \sigma_{pp}/dydp_T}, \quad (1)$$

where $\langle N_{bin} \rangle$ is the average number of binary nucleon-nucleon (NN) collisions per event, and $\langle N_{bin} \rangle / \sigma_{pp}^{inel}$ is the nuclear overlap function $T_A(b)$ [11,12]. The value of σ_{pp}^{inel} is taken to be 42 mb.

The left panel of Fig. 3 shows R_{dAu} values for charged pions ($(\pi^+ + \pi^-)/2$) in minimum bias and 0-20% central collisions at $|y| < 0.5$. The R_{dAu} for 0-20% central collisions are higher than R_{dAu} for minimum bias collisions. The result $R_{dAu} > 1$ indicates a slight enhancement of high p_T charged pion yields in $d+Au$ collisions compared to binary collision scaled charged pion yields in $p+p$ collisions within the measured (y, p_T) range. The right panel of Fig. 3 shows the R_{dAu} of baryons ($p+\bar{p}$) for the minimum bias collisions at $|y| < 0.5$.

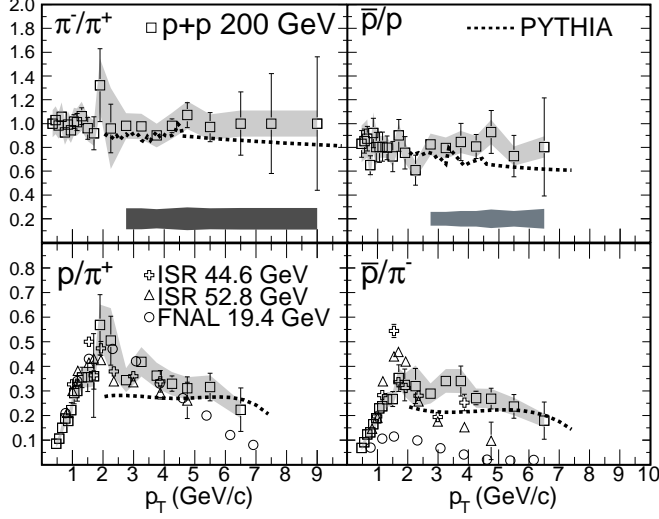


Fig. 4. Ratio of π^-/π^+ , \bar{p}/p , p/π^+ , \bar{p}/π^- at midrapidity ($|y| < 0.5$) as a function of p_T in $p+p$ minimum bias collisions. For comparison the results from lower energies at ISR [26] and FNAL [27] are also shown for p/π^+ and \bar{p}/π^- ratios. The dotted curves are the results from PYTHIA. The shaded bands below the π^-/π^+ and \bar{p}/p ratios are the point-to-point correlated errors in the yields associated with the ratio.

The R_{dAu} for $p+\bar{p}$ is again greater than unity for $p_T > 1.0$ GeV/c and is larger than R_{dAu} for charged pions. The R_{dAu} of pions for $2 < p_T < 5$ GeV/c is 1.24 ± 0.13 and that for $p+\bar{p}$ is 1.49 ± 0.17 in minimum bias collisions. Identified hadron R_{dAu} are sensitive to nuclear modification of the PDF from processes such as nuclear shadowing and parton saturation as well as to transverse momentum broadening, energy loss in cold nuclear matter and hadronization through recombination, thereby further constraining the models [23].

4 Particle ratios

The particle ratios at midrapidity as a function of p_T for $p+p$ and $d+Au$ minimum bias collisions are shown in Figs. 4 and 5 respectively. Correlated errors are shown as the shaded bands below the data points. The π^-/π^+ -ratio has a value ~ 1 and is independent of p_T in both $p+p$ and $d+Au$ collisions. The \bar{p}/p -ratio for $p+p$ collisions is also independent of p_T within the range studied and has a value of 0.81 ± 0.1 at $2.5 < p_T < 6.5$ GeV/c. However, in $d+Au$ collisions we observe a clear decrease of \bar{p}/p for $p_T > 6$ GeV/c. In quark fragmentation, the leading hadron is more likely to be a particle rather than an anti-particle, and there is no such preference from a gluon jet. A decrease in the antiparticle/particle ratio with p_T would then indicate a significant quark jet contribution to the baryon production. It is, however, not clear whether the same effect exists in $p+p$ collisions or whether the decrease of \bar{p}/p is due to additional nuclear effects in $d+Au$ collisions. Calculations from

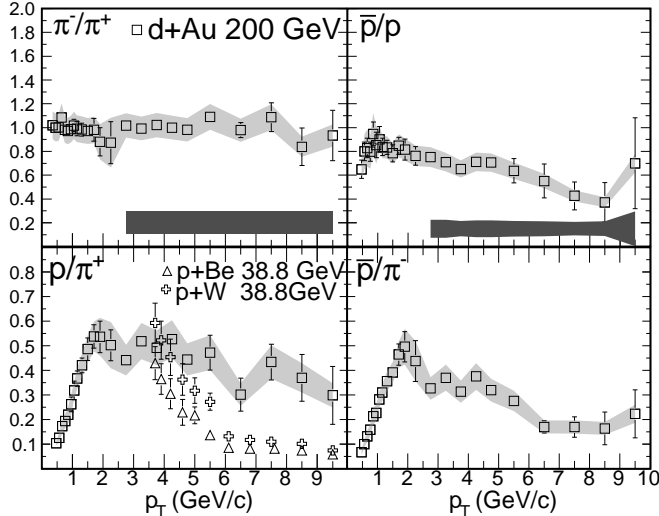


Fig. 5. Same as Fig. 4 for $d+Au$ minimum bias collisions. For comparison the p/π^+ -ratio from lower energies at FNAL [27] are shown.

PYTHIA(v6.319) predict somewhat more prominent p_T -dependence [15].

At RHIC, the p/π^+ and \bar{p}/π^- ratios increase with p_T up to 2 GeV/ c and then start to decrease for higher p_T in both $p+p$ and $d+Au$ collisions. The \bar{p}/π^- -ratio rapidly approaches a value of 0.2, which is between the values in e^+e^- collisions for quark and gluon jets [24,25]. The p/π^+ and \bar{p}/π^- ratios from PYTHIA are constant at high p_T in contrast to a decreasing trend observed in the data. The p/π^+ -ratios in $p+p$ collisions compare well with results from lower energy ISR and FNAL fixed target experiments [26,27]. Meanwhile, \bar{p}/π^- -ratios at high p_T have a strong energy dependence with larger values at higher beam energies. In $d+Au$ collisions the p/π^+ -ratio at high p_T is lower for $p+A$ collisions at FNAL energy than at RHIC.

5 Comparison to NLO pQCD and model calculations

In Fig. 6 we compare $(\pi^+ + \pi^-)/2$ and $(p+\bar{p})/2$ yields in minimum bias $p+p$ and $d+Au$ collisions at midrapidity for high p_T to those from NLO pQCD calculations and the phenomenological parton model (EPOS) [28]. The results from EPOS agree fairly well with our data for charged pions and proton+anti-proton in $p+p$ and $d+Au$ collisions. The NLO pQCD results are based on calculations performed with two sets of FFs, the *Kniehl-Kramer-Potter (KKP)* [29] and the *Albino-Kniehl-Kramer (AKK)* set of functions [30]. The factorization scale for all the NLO pQCD calculations shown is for $\mu = p_T$. The charged pion data for $p_T > 2$ GeV/ c in $p+p$ collisions are reasonably well described by the NLO pQCD calculations using the KKP and AKK set of FFs. A similar observation for π^0 s using KKP FFs was made by the PHENIX

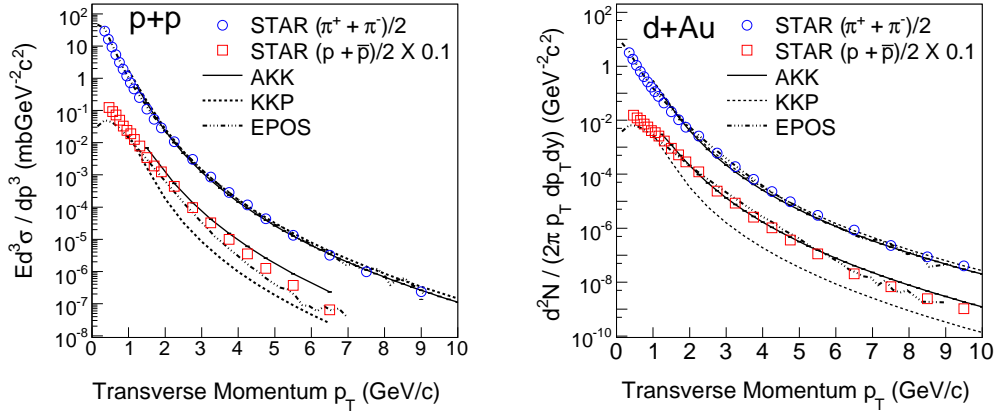


Fig. 6. Midrapidity invariant yields for $(\pi^+ + \pi^-)/2$ and $(p+\bar{p})/2$ at high p_T for minimum bias $p+p$ and $d+Au$ collisions compared to results from NLO pQCD calculations using KKP [29] (PDF: CTEQ6.0) and AKK [30] (PDF: CTEQ6M) sets of fragmentation functions and results from the EPOS model [28]. The PDFs for d and Au-nucleus are taken from Refs. [31] and [32] respectively. All results from NLO pQCD calculations are with factorization scale is $\mu = p_T$.

Collaboration [33]. For $d+Au$ collisions NLO pQCD calculations with KKP FFs are consistent with the data for $p_T > 4$ GeV/ c while those with AKK FFs underpredict the measured charged pion yields.

The proton+anti-proton yield at high p_T in $p+p$ and $d+Au$ collisions is much higher than the results from NLO pQCD calculations using the KKP set of FFs and lower compared to calculations using AKK FFs. The relatively better agreement of NLO pQCD calculations with AKK FFs compared to those with KKP FFs for proton+anti-proton yields shows the importance of the flavor-specific measurements in e^+e^- collisions in determining the FFs for baryons. One may further improve the NLO pQCD calculations by an all-order resummation of large logarithmic corrections to the partonic cross-sections [34].

6 Scaling of particle production

The invariant cross-sections of inclusive pion production in high energy $p+p$ collisions have been found to follow the scaling laws [36] :

$$E \frac{d^3\sigma}{dp^3} = \frac{1}{p_T^n} f(x_T) \quad \text{or} \quad E \frac{d^3\sigma}{dp^3} = \frac{1}{\sqrt{s}^n} g(x_T) \quad (2)$$

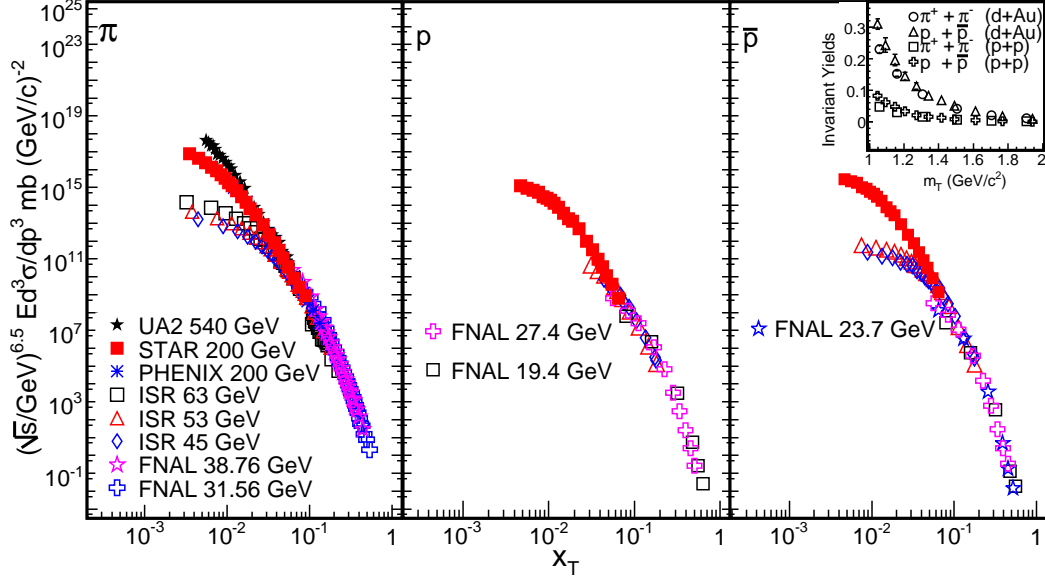


Fig. 7. x_T -scaling of pions, protons and anti-protons. The data from other experiments are from the following references, FNAL : Refs [27,35], ISR : Ref. [26], PHENIX : Ref. [33], and UA2 [40]. The inset shows the m_T -scaling of the invariant yields for charged pions and protons+anti-protons in $p+p$ and $d+Au$ collisions.

where $x_T = 2p_T/\sqrt{s}$ and $f(x_T)$ and $g(x_T)$ are some functions of x_T . Similar scaling has been observed in $e^+ + e^-$ collisions, but without the \sqrt{s}^n or p_T^n factor [37]. The value of the power n ranges from 4 to 8 [38]. In the general scaling form $\sim 1/p_T^n$, n depends on the quantum exchanged in the hard scattering. In parton models, it is related to the number of point-like constituents taking an active role in the interaction. The value reaches 8 in the case of a quark-meson scattering by exchanging a quark. With the inclusion of QCD, the scaling law follows as $\sim 1/\sqrt{s}^n$, where n becomes a function of x_T and \sqrt{s} . The value of n depends on the evolution of the structure function and FFs. $n=4$ is expected in more basic scattering processes (as in QED) [38,39].

Figure 7 shows the x_T -scaling of pions, protons and anti-protons. The value of n obtained for the scaling with \sqrt{s}^n of the invariant cross-section is 6.5 ± 0.8 . The STAR data covers the range $0.003 < x_T < 0.1$. The data points deviate from the scaling behavior for $p_T < 2$ GeV/c for pions and protons, which could be interpreted as a transition region from soft to hard processes in the particle production. The deviations start at a higher p_T for the anti-protons. The available data on pion and proton invariant cross-sections at various center-of-mass energies [26,27,33,35,36,40] for $p_T > 2$ GeV/c are compiled and fitted using the function $\frac{1}{p_T^n} (1 - x_T)^m$. The value of n ranges from 6.0 to 7.3 for $\sqrt{s_{NN}}$ between 19 GeV and 540 GeV, while that for m ranges between 13 and 22. The average value of n for pions is 6.8 ± 0.5 and that for protons and anti-protons is 6.5 ± 1.0 . The variations in n and m values may lead to differences in details of scaling behaviour at different energies when the

cross-section is multiplied by $1/p_T^n$ [41]. This feature is not observed in the scaling shown in Fig. 7 due to the data spanning several orders of magnitude. The inset of Fig. 7 shows the m_T scaling at $p_T < 2$ GeV/ c , consistent with possible transition between soft and hard processes at around $p_T \simeq 2$ GeV/ c . The m_T -scaling also indicates that flow effects in $p+p$ and $d+Au$ collisions are negligible [4,5]. The presented data suggests that the transition region from soft to hard physics occurs around $p_T \sim 2$ GeV/ c in $p+p$ collisions.

7 Summary

We have presented transverse momentum spectra for identified charged pions, protons and anti-protons from $p+p$ and $d+Au$ collisions at $\sqrt{s_{NN}} = 200$ GeV. The transverse momentum spectra are measured around midrapidity ($|y| < 0.5$) over the range of $0.3 < p_T < 10$ GeV/ c with particle identification from the ionization energy loss and its relativistic rise in the Time Projection Chamber, as well as the Time-of-Flight in STAR. The following conclusions can be drawn from the present study: (a) The nuclear modification factor around midrapidity is enhanced in $d+Au$ collisions to about 1.5 for pions and to about 2 for protons and antiprotons at intermediate p_T ($2 < p_T < 5$ GeV/ c). (b) Identified particle ratios were measured up to p_T of 7 GeV/ c in $p+p$ and 10 GeV/ c in $d+Au$ reactions. Their dependence on species, p_T and collisions energy was shown to be sensitive to the relative contributions from quark and gluon fragmentation as well as to their fragmentation functions. (c) The NLO pQCD calculations describe the high p_T data for charged pions reasonably well in $p+p$ collisions and $d+Au$ collisions. In general, baryon production has historically been difficult to describe by pQCD and hadronization [39,42]. Use of the recently published AKK FFs results in a much improved description of the measured p and \bar{p} spectra. (d) The proton and pion spectra in $p+p$ collisions follow x_T -scaling with a beam-energy dependent factor $\sim \sqrt{s_{NN}}^{6.5}$ above $p_T \sim 2$ GeV/ c . The pion and proton spectra follow transverse mass scaling for $m_T < 2$ GeV/ c^2 in both $p+p$ and $d+Au$ collisions, suggesting the transition region from soft to hard process domination occurs at $p_T \sim 2$ GeV/ c in these collision systems. The measurements presented in this paper provide better constraints on jet quenching and quark recombination models which are presently the best candidates for explaining particle production in the intermediate p_T region.

We would like to thank Simon Albino, Stefan Kretzer and Werner Vogelsang for providing us the NLO pQCD results, Klaus Werner for the EPOS results and J. Raufeisen for useful discussions. We thank the RHIC Operations Group and RCF at BNL, and the NERSC Center at LBNL for their support. This work was supported in part by the HENP Divisions of the Office of Science of the U.S. DOE; the U.S. NSF; the BMBF of Germany; IN2P3, RA, RPL, and EMN of France; EPSRC of the United Kingdom; FAPESP of Brazil;

the Russian Ministry of Science and Technology; the Ministry of Education and the NNSFC of China; IRP and GA of the Czech Republic, FOM of the Netherlands, DAE, DST, and CSIR of the Government of India; Swiss NSF; the Polish State Committee for Scientific Research; STAA of Slovakia, and the Korea Sci. & Eng. Foundation.

References

- [1] J. C. Collins and D. E. Soper, *Ann. Rev. Nucl. Part. Sci.* 37 (1987) 383; J. C. Collins, D. E. Soper and G. Sterman in *Perturbative Quantum Chromodynamics* (World Scientific, 1989) edited by A. H. Muller and *Adv. Ser. Direct. High Energy Phys.* 5 (1988) 1; G. Sterman et al., *Rev. Mod. Phys.* 67 (1995) 157.
- [2] R. D. Field and R. P. Feynman, *Nucl. Phys. B* 136 (1978) 1; J. F. Owens, *Rev. Mod. Phys.* 59 (1987) 465.
- [3] D. E. Soper, *Nucl. Phys. B (Proc. Suppl.)* 53 (1997) 69; A. D. Martin, W. J. Stirling and R.G. Roberts, *Phys. Lett. B* 354 (1995) 155; M. Gluck, E. Reya and A. Vogt, *Z. Phys. C* 67 (1995) 433; H. L. Lai et al., *Phys. Rev. D* 51 (1995) 4763.
- [4] BRAHMS Collaboration, I. Arsene et al., *Nucl. Phys. A* 757 (2005) 1; PHOBOS Collaboration, B.B. Back et al., *Nucl. Phys. A* 757 (2005) 28; STAR Collaboration, J. Adams et al., *Nucl. Phys. A* 757 (2005) 102; PHENIX Collaboration, K. Adcox et al., *Nucl. Phys. A* 757 (2005) 184.
- [5] D. Teaney, J. Lauret, E.V. Shuryak, arXiv:nucl-th/0110037.
- [6] V. Greco, C.M. Ko and P. Levai, *Phys. Rev. Lett.* 90 (2003) 202302; R. J. Fries, B. Muller, C. Nonaka and S. A. Bass, *Phys. Rev. Lett.* 90 (2003) 202303.
- [7] STAR Collaboration, C. Adler et al., *Phys. Rev. Lett.* 90 (2003) 082302; PHENIX Collaboration, S.S. Adler et al., *Phys. Rev. Lett.* 91 (2003) 072301.
- [8] STAR Collaboration, J. Adams et al., *Phys. Rev. Lett.* 92 (2004) 052302.
- [9] X.-N. Wang and M. Gyulassy, *Phys. Rev. Lett.* 68 (1992) 1480.
- [10] K. H. Ackerman et al., *Nucl. Instrum. Meth. A* 499 (2003) 624.
- [11] STAR Collaboration, J. Adams et. al, *Phys. Rev. Lett.* 91 (2003) 072304; *Phys. Rev. C.* 70 (2004) 064907;
- [12] STAR Collaboration, J. Adams et. al, *Phys. Rev. Lett.* 92 (2004) 112301.
- [13] S. N. White, arXiv:nucl-ex/0507023.
- [14] STAR Collaboration, J. Adams et al., *Phys. Rev. Lett.* 91 (2003) 172302.

- [15] T. Sjostrand et al., *Comput. Phys. Commun.* 135 (2001) 238.
- [16] G. Corcella et al., *JHEP* 0101 (2001) 010.
- [17] A. Drees and Z. Xu, *Proceedings of the Particle Accelerator Conference 2001, Chicago, IL*, p. 3120.
- [18] STAR Collaboration, J. Adams et. al, *Phys. Lett. B* 616 (2005) 8.
- [19] M. Shao et al., arXiv:nucl-ex/0505026.
- [20] H. Bichsel, *Proceedings of 8th International Conference on Advance Technology and Particle Physics*, ICATPP 2003, p. 448.
- [21] M. Heinz (for STAR Collaboration), *J. Phys. G* 31 (2005) S1011.
- [22] STAR Collaboration, J. Adams et. al, *Phys. Rev. C* 71 (2005) 064902; G. Wilk and Z. Wlodarczyk, *Phys. Rev. Lett.* 84 (2000) 2770.
- [23] R. Vogt, *Phys. Rev. C* 70 (2004) 064902; J. Qiu and I. Vitev, arXiv:hep-ph/0405068; D. Kharzeev, Y. Kovchegov and K. Tuchin, *Phys. Lett. B* 599 (2004) 23; R. C. Hwa and C.B. Yang, *Phys. Rev. Lett.* 93 (2004) 082302.
- [24] DELPHI Collaboration, P. Abreu et al., *Eur. Phys. J. C* 5 (1998) 585; *Eur. Phys. J. C* 17 (2000) 207.
- [25] OPAL Collaboration, G. Abbiendi et al., *Eur. Phys. J. C* 16 (2000) 407.
- [26] British-Scandinavian Collaboration, B. Alper et al., *Nucl. Phys. B* 100 (1975) 237.
- [27] E706 Collaboration, L. Apanasevich et al., *Phys. Rev. D* 68 (2003) 052001; P. B. Straub et al., *Phys. Rev. D* 45 (1992) 3030.
- [28] K. Werner, F. Liu and T. Pierog, arXiv:hep-ph/0506232. The EPOS model includes two important nuclear effects through elastic and inelastic parton ladder splitting. The elastic splitting is related to screening and saturation while the inelastic splitting is related to the hadronization process. The proton+anti-proton spectra from EPOS model is not corrected for the hyperon feed-down corrections.
- [29] B. A. Kniehl, G. Kramer and B. Potter, *Nucl. Phys. B* 597 (2001) 337. The KKP FFs are obtained from e^+e^- collision data where the observed hadron is identified as a π^\pm or K^\pm or $p(\bar{p})$ and the emitting parton is identified as either a gluon, light (u, d , and s) quark, c quark or b quark.
- [30] S. Albino, B. A. Kniehl and G. Kramer, *Nucl. Phys. B* 725 (2005) 181. The AKK FFs use the recent data from the OPAL Collaboration [25] on light-flavor separated measurements of light charged hadron production in e^+e^- collisions, thereby allowing the extraction of the flavor-dependent FFs of light quarks.
- [31] B. A. Kniehl and L. Zwirner, *Nucl. Phys. B* 637 (2002) 311. For NLO pQCD calculations in $d+Au$ collisions, the parton distributions for the deuteron are obtained via the average of the distributions in protons and neutrons ($(p+n)/2$).

- [32] L. Frankfurt, V. Guzey and M. Strikman, Phys. Rev. D 71 (2005) 054001; D. de Florian and R. Sassot, Phys. Rev. D 69 (2004) 074028. The parton distributions for gold nuclei are obtained by convoluting the free nucleon parton densities with simple weight functions that are meant to parametrize nuclear effects. These are further constrained by comparing to deep inelastic scattering data off nuclei.
- [33] PHENIX Collaboration, S.S. Adler et al, Phys. Rev. Lett. 91 (2003) 241803.
- [34] D. de Florian and W. Vogelsang, Phys. Rev. D 71 (2005) 114004.
- [35] D. Antreasyan et al., Phys. Rev. D 19 (1979) 764.
- [36] A. G. Clark et al., Phys. Lett. B 74 (1978) 267; CCOR Collaboration, A. L. S. Angelis et al., Phys. Lett. B 79 (1978) 505; PHENIX Collaboration, S.S. Adler et al., Phys. Rev. C 69 (2004) 034910.
- [37] TPC Collaboration, H. Aihara et al., Phys. Rev. Lett. 61 (1988) 1263; ALEPH Collaboration, D. Buskulic et al., Z. Phys. C 66 (1995) 355; ARGUS Collaboration, H. Albrecht et al., Z. Phys. C 44 (1989) 547.
- [38] S. M. Berman, J. D. Bjorken and J. B. Kogut, Phys. Rev. D 4 (1971) 3388; R. Blankenbecler, S. J. Brodsky and J.F. Gunion, Phys. Lett. B 42 (1972) 461; J.F. Owens, E. Reya, M. Gluck, Phys. Rev. D 18 (1978) 1501.
- [39] S. Ekelin and S. Fredriksson, Phys. Lett. B 149 (1984) 509.
- [40] UA2 Collaboration, M. Banner et al., Phys. Lett. B 115 (1982) 59.
- [41] S. J. Brodsky, H. J. Pirner and J. Raufeisen, arXiv:hep-ph/0510315.
- [42] X. Zhang, G. Fai, and P. Levai, Phys. Rev. Lett. 89 (2002) 272301; B. Andersson, G. Gustafson, T. Sjostrand, Phys. Scripta 32 (1985) 574; Nucl. Phys. B 197 (1982) 45.